J Mol Model (2013) 19:4701–4711
DOI 10.1007/s00894-012-1507-z

ORIGINAL PAPER

Interaction of organic solvents with protein structures at protein-solvent interface

Morteza Khabiri · Babak Minofar · Jan Brezovský · Jiří Damborský · Rudiger Ettrich

Received: 25 December 2011 / Accepted: 13 June 2012 / Published online: 4 July 2012

Abstract The effect of non-denaturing concentrations of three different organic solvents, formamide, acetone and isopropanol, on the structure of haloalkane dehalogenases DhaA, LinB, and DbjA at the protein-solvent interface was studied using molecular dynamics simulations. Analysis of B-factors revealed that the presence of a given organic solvent mainly affects the dynamical behavior of the specificity-determining cap domain, with the exception of DbjA in acetone. Orientation of organic solvent molecules on the protein surface during the simulations was clearly dependent on their interaction with hydrophobic or hydrophilic surface patches, and the simulations suggest that the behavior of studied organic solvents in the vicinity of hyrophobic patches on the surface is similar to the air/water interface. DbjA was the only dimeric enzyme among studied haloalkane dehalogenases and provided an opportunity to explore effects of organic solvents on the quaternary structure. Penetration and trapping of organic solvents in the network of interactions between both monomers depends on the physico-chemical properties of the organic solvents. Consequently, both monomers of this enzyme oscillate differently in different organic solvents. With the exception of LinB in acetone, the structures of studied enzymes were stabilized in water-miscible organic solvents.

Keywords Molecular dynamics · Non-aqueous media · Organic solvents · Solvent orientation

M. Khabiri · B. Minofar · R. Ettrich (✉)
Institute of Nanobiology and Structural Biology of GCRC,
Academy of Sciences of the Czech Republic,
Zamek 136,
373 33 Nove Hrady, Czech Republic
e-mail: ettrich@nh.cas.cz

M. Khabiri · R. Ettrich
Faculty of Sciences, University of South Bohemia in Ceske Budejovice,
Zamek 136,
373 33 Nove Hrady, Czech Republic

J. Brezovský · J. Damborský
Loschmidt Laboratories, Department of Experimental Biology and Research Centre for Toxic Compounds in the Environment,
Faculty of Science, Masaryk University,
Kamenice 5/A13,
625 00 Brno, Czech Republic

J. Brezovský · J. Damborský
International Clinical Research Center, St. Anne's University Hospital Brno,
Pekarska 53,
656 91 Brno, Czech Republic

Introduction

A wide range of chemical agents used in industrial and agricultural activities are released into the environment as chemical contaminants. A large number of these compounds belong to haloalkanes. Several organisms produce various enzymes which are able to hydrolytically cleave the carbon-halogen bond in halogenated compounds like halogenated alkanes, cycloalkanes and alcohols [1–3]. These enzymes are called haloalkane dehalogenases (HLDs), and they belong to the α/β-hydrolase protein superfamily [4]. They use a hydrolytic mechanism to transform haloalkane into an organic halide ion and an alcohol. Structurally these enzymes are comprised of two different domains [5]. The larger, so-called main domain is conserved in all α/β-hydrolases and contains a central β-sheet. The smaller domain is less conserved within the α/β−fold superfamily, and is called cap domain. The active site is located between these two domains in an internal hydrophobic cavity and can be reached through a tunnel to the bulk of the solvent [4–6].

Potential application of HLDs for decontamination of environmental pollutants makes them interesting targets

for medium engineering to improve their catalytic efficiency [7]. Three HLDs with known crystal structure and different substrate specificity were selected for this study; DbjA from *Bradyrhizobium japonicum* USDA110 [8], DhaA from *Rhodococcus rhodochrous* NCIMB 13064 [9], and LinB from *Sphingomonas paucimobilis* UT26 [10]. The substrate specificities of these HLDs are mainly due to differences in the geometry and the composition of the active site, and the entrance tunnel connecting the active site to the protein surface (Fig. 1; [11]). Recently, it has been shown experimentally that the activity of these three enzymes is significantly affected by the nature and concentration of different organic solvents [12].

Water is the essential solvent for life, and so far the water exclusive properties and its unique capabilities as a solvent have drawn broad attention in biochemistry, while inability of this unique solvent to solvate many non-polar molecules were not considered [13, 14]. It is expected that mixing of water with water miscible solvents such as organic solvents could compensate for some of the shortcomings in water properties [15]. The main advantages of mixtures of water with organic solvents can be summarized as: (1) speed up general reaction rates, (2) provide an environment for reactions in which hydrophobic interactions are involved in the complex formation between enzyme and substrate and (3) overcome unwanted water-dependent side reactions [1, 16, 17]. Changing the reaction media from physiological to non-physiological ones influences the structure and function of the enzyme. The solvent accessible surface of the enzyme is in the first place influenced by changing the reaction media. Many studies show that addition of organic solvents to enzyme water solutions decreases the number of water molecules in the first solvation shell of the protein [18, 19]. In fact, organic molecules repel water molecules from the surface. Consequently, polar amino acid side chains become more rigid, and prefer favorable interactions with other amino acids inside the protein structure. In contrast, non-polar amino acid side chains become more flexible. It has been shown that reorientation of polar amino acid side chains from the surface to the core increases the total number of hydrogen bonds and salt bridges inside the enzyme structure, making it more rigid in comparison to the enzyme structure in pure water media [18–20]. Moreover, it has been shown that the amount of water molecules on the enzyme surface in non-aqueous media is one of the key factors for enzyme stability [21]. Taken together, we can say that the effect of organic solvents on enzyme structure depends on the physicochemical property of amino acids located on the protein surface and the physicochemical property of organic solvent.

While the general fold of a protein is determined and preserved by intra-molecular interactions, as are hydrophobic, van der Waals, hydrogen bonding and electrostatic interactions [22], solvent molecules are crucial for the extra-molecular hydrophobic interactions and dynamic behavior of the enzyme. In solution both, enzyme and solvent, have mutual effects. Hereby, not only do general media properties influence the overall enzyme structure, but also particular solvent molecules close to the protein surface can have specific interactions with the enzyme. Therefore, the nature of the enzyme surface determines solvent interaction and structure in its vicinity. Adding organic solvent molecules that have a dual nature of both, hydrophobic and hydrophilic properties, to the water changes its properties as a physiological solvent [23, 24]. These organic solvents are considered as co-solvents, which enhance hydrophobicity of the medium, i.e., reducing its polarity and hence dielectric constant.

In this work, we investigated the effect of three selected organic solvents/-water mixtures, formamide 5 %, acetone 10 %, and isopropanol 20 %, on the tertiary structure of DhaA, LinB, and DbjA and the quaternary structure of DbjA, with special focus on the behavior of these organic solvents at the protein surface.

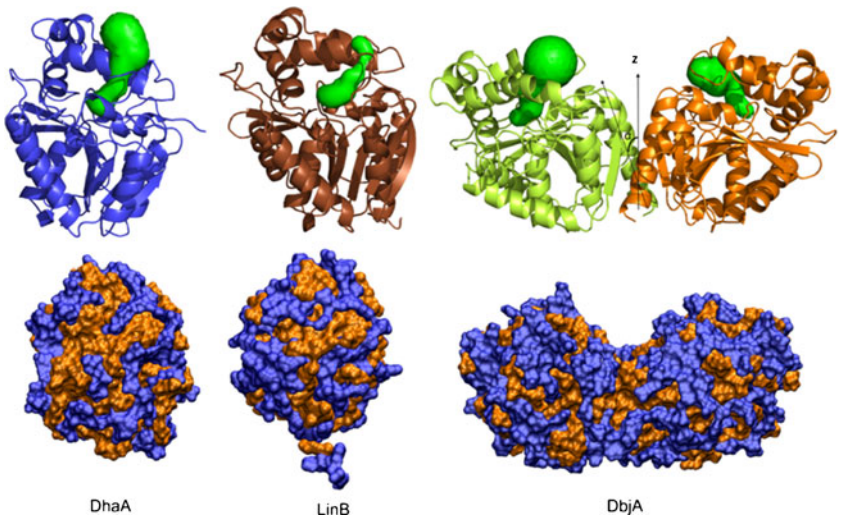

Fig. 1 3-D models of the crystal structures of dehalogenases DhaA (PDB ID 1CQW), LinB (PDB ID 1 MJ5) and DbjA (PDB ID 3A2M). Structures are represented by ribbons (*top*) and molecular surfaces (*bottom*). Tunnels connecting the active site with bulk solvent are shown in *green*. Hydrophobic surface patches are in *orange* and hydrophilic surface patches are in *blue*. The tunnels were calculated by CAVER [46] and structures were visualized in Pymol [39]

Methods

Molecular dynamics

Three-dimensional structures of the organic molecules were optimized, and partial charges were calculated in Gaussian 03 employing the Hartree-Fock method and the 6-31 G* basic set [25]. Geometries were optimized at the MP2/6-31 G* level. Topologies of all organic molecules were generated using MKTOP [26] for the all atom optimized potentials for liquid simulation (OPLSAA) force field [27–29]. Three different mixtures of organic co-solvents with water [formamide 5 % (v/v), acetone 20 % (v/v) and isopropanol 10 % (v/v)] were prepared to match the experimental conditions according to Stepankova et al. [12].

Optimizing of the structures of organic solvents was necessary as the atomic partial charges were not available for all molecules in the OPLS force field database but for other parameters such as the Lennard Jones potential parameters we have used the OPLS all atom parameters. The parameters for the studied molecules are tabulated in Table 1 with their OPLS number, partial charge, sigma and epsilon values.

Crystal structure coordinates for DhaA (PDB ID: 1CQW), DbjA (PDB ID: 3A2M) and LinB (PDB-ID: 1 MJ5) were downloaded from the Protein Data Bank and V172A, I209L and G292A substitutions were introduced to the structure of DhaA to match the primary structure of the enzyme from *Rhodococcus rhodochrous* NCIMB13064 [30] using YASARA structure [31].

During the setup of the molecular dynamics simulations, crystallographic water molecules were kept in place. The ionization state of protonable residues of all three enzymes was considered the same as the ionization state observed in water according to the pH memory phenomenon described by Klibanov [15].

Initially, all crystal structures were energy minimized *in vacuo* using a short steepest descent protocol for at least 1000 step. The minimized crystal structures were then solvated in pre-equilibrated extended simple point-charge (SPCE) water [32], formamide 5 % (v/v), isopropanol 10 % (v/v) and acetone 20 % (v/v) in a rectangular box with a minimum distance of 1.5 nm between the protein and the box edges. For each organic solvent solution the pre-equilibration constituted 200 ns of MD simulation to fully equilibrate the water-solvent mixture. After solvation of the protein, sodium counter ions were added by replacing water molecules to provide a neutral simulation box. All atoms were given an initial velocity obtained from a Maxwellian distribution at the desired initial temperature. In all simulations, the proteins were restraint for 2 ns with a force constant of 1000 kJ mol^{-1} nm^{-2} to allow the water and organic solvents to relax until the solvents get optimized around the protein. After relaxation, the position restraints on the protein were removed, and the system was further equilibrated by gradually heating from 290 K to 300 K during 50 ps simulation. Production runs were performed for 35 ns. Different MD simulations with different initial states were performed to test the ergodicity of the system. MD simulations were started with three different initial temperatures, 280 K, 290 K and 310 K. A second series of MD simulations was interrupted every 5 ns to assign new velocities according to a Maxwell-Boltzmann distribution to the last snapshot to create a new initial state. The simulations were then continued for another 5 ns until they reached an overall length of 40 ns. In all cases, the simulations lead to the same results and the RMSD of the proteins reached a stable plateau after 10 or max 15 ns, demonstrating the

Table 1 Force field parameters used for the different solvent molecules

Molecule	OPLS number	Atom	Charge	sigma (nm)	epsilon (kJ/mol)
Acetone	opls_280	C (C=O)	0.68880	3.75E-01	4.39320E-01
	opls_135	C (CH3)	-0.22867	3.50E-01	2.76144E-01
	opls_281	O (C=O)	-0.59752	2.96E-01	8.78640E-01
	opls_282	H (CH3)	0.06101	2.42E-01	6.27600E-02
Formamide	opls_280	O (CHO)	-0.46900	2.96E-01	8.78640E-01
	opls_135	C (CHO)	0.58250	3.75E-01	4.39320E-01
	opls_281	H (CHO)	0.03710	2.42E-01	6.28000E-02
	opls_237	N (NH2)	-0.85730	3.25E-01	7.11280E-01
	opls_240	H (NH2)	0.40400	0.00E+00	0.00000E+00
Isopropanol	opls_154	O (OH)	-0.68162	3.12E-01	7.11280E-01
	opls_155	H (OH)	0.39095	0.00E+00	0.00000E+00
	opls_158	C (OH)	0.43635	3.50E-01	2.76144E-01
	opls_135	C (CH3)	-0.31100	3.50E-01	2.76144E-01
	opls_140	H (CH3)	0.08244	2.50E-01	1.25520E-01

ergodicity of the system. All simulations and analysis of the trajectories were performed in GROMACS 3.3.3 [33, 34] with an extended OPLSAA force field [28]. The isothermal isobaric ensemble (NPT) was used. The temperature was maintained at 300 K and the pressure was maintained at 1 bar with a compressibility of 4.6×10^{-5}/bar by weak coupling to temperature and pressure baths using the Berendsen method [35] with relaxation times of 0.1 ps. Van der Waals forces were evaluated with a Lennard-Jones potential having 10 Å cut-off, and long-range electrostatic contributions were evaluated using the particle mesh Ewald method [36] with a direct interaction cut-off of 10.0 Å. A time step of 0.002 ps was employed. Lengths of all covalent bonds were constrained by the linear constraint solver algorithm [37]. All simulations were run with periodic boundary conditions. The temperature factors (B-factors) were calculated from the root mean square fluctuations using the g_rmsf command in Gromacs with the option -ox, which uses the equation $B=(8\pi^2\times RMSF^2)/3$. Molecular graphics images were produced using VMD [38] and PyMOL [39]. The graphs were prepared in XMgrace (http://plasma-gate.weizmann.ac.il/Grace/).

Results and discussion

Solvation shell surrounding protein structures

Water solvation shell around three studied enzymes is not homogenous and shows clear preferences of water and solvent molecules for different places on the protein surfaces. This is in sharp contrast to the homogenous mixture of organic solvent and water in the bulk solvent. Table 2 shows the percentage of hydrophobic and hydrophilic surface area of DhaA, LinB and DbjA which is covered with water or different organic solvents. A closer look at the first hydration shell of solvated enzyme in pure water and the water/organic solvent mixtures shows that water molecules are repelled from the enzyme surfaces and replaced by organic solvents in the latter case. This is in agreement with the data reported by Soares et al. [19]. However, the distribution is not flat and population maps of formamide, acetone and isopropanol on the surface of the three enzymes show organic solvent molecules to be populated mainly on hydrophobic patches of the surface of DhaA, LinB and DbjA. Distribution of water and organic solvent molecules surrounding the DbjA surface in formamide, acetone and isopropanol is shown in Fig. 2. While organic solvent molecules accumulate on hydrophobic patches, water molecules are mainly distributed over hydrophilic patches on the surfaces. The distribution of water and organic solvent molecules around the molecular surface of LinB and DhaA is very similar to each other (data not shown).

Orientation of organic solvents in the vicinity of hydrophobic patches

The radial distribution function (RDF) is a good parameter to study orientation of surrounding solvent molecules around a solute [40]. We calculated the RDF of solvent molecules relative to hydrophobic amino acids at the border between a hydrophobic and hydrophilic patch. At the surface of all three HLDs, the formamide HCO group prefers to stick to the hydrophobic patch while its amide group is oriented toward the solution (Fig. 3). This

Table 2 Percentage of hydrophobic and hydrophilic area of DhaA, LinB and DbjA covered by organic solvents and water, respectively

Enzyme	Solvents	% hydrophobic area covered by organic solvents	% hydrophilic area covered by organic solvents	% hydrophobic area covered by water	% hydrophilic area covered by water
DhaA	acetone	27.70±0.5	11.43±0.5	24.03±0.6	67.99±0.5
	isopropanol	19.31±0.5	7.71±0.5	24.87±0.5	68.68±0.4
	formamide	16.32±0.5	6.88±0.5	25.58±0.8	69.84±0.6
	water	NA	NA	26.33±0.5	73.94±0.4
LinB	acetone	23.69±0.5	10.92±0.5	20.88±0.5	70.09±0.3
	isopropanol	18.33±0.6	12.18±0.6	22.83±0.5	73.86±0.5
	formamide	16.10±0.8	12.18±0.5	22.98±0.5	74.06±0.5
	water	NA	NA	27.18±0.5	81.04±0.5
DbjA	acetone	24.78±0.8	14.72±0.4	17.80±0.4	61.97±0.8
	isopropanol	22.02±0.7	10.39±0.5	19.69±0.5	65.99±0.6
	formamide	19.15±0.5	9.73±0.5	20.07±0.5	68.13±0.8
	water	NA	NA	24.97±0.5	74.27±0.6

NA – not applicable

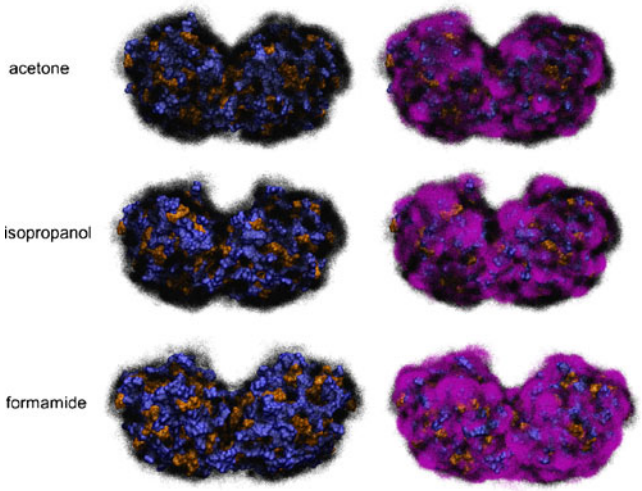

Fig. 2 Occupation of organic solvents and water on the surface of DbjA during 35 ns of MD simulation. Organic solvents are shown as *black* (*left*) and water as *violet* (*right*) dots. Hydrophobic surface patches are *orange* and hydrophilic surface patches are *blue*. The organic solvents occupy primarily the hydrophobic regions, while the water occupy primarily the hydrophilic regions. Structures were visualized in Pymol [39]

result is consistent with studies by vibrational sum frequency generation spectroscopy at the air-water interface, showing that formamide preferentially points toward the vapor phase with its HCO group [41, 42]. Although formamide can react chemically with amines, under the chosen conditions, low concentration of the co-solvent, low temperature and neutral pH 7, we do not expect a reaction to take place to a larger extend, and therefore our classical MD simulations properly described the behavior of the system in the time-frame of the tens of nanoseconds. In the case of acetone, we did not observe any specific preference in the orientation of either the methyl (CH3) or carbonyl (C=O) groups. Instead, its carbonyl and one of its methyl groups were oriented toward the surface at the same time (Fig. 3). Since the positions of the two methyl groups in the acetone molecules are equally weighted, both acetone methyl groups were oriented toward the surface with the same frequency, and in the RDF graph we observe no difference between carbonyl and methyl groups close to the hydrophobic surfaces. Interestingly, the behavior of the solvents in the vicinity of the protein is very similar to the behavior observed for solvents at the air-water

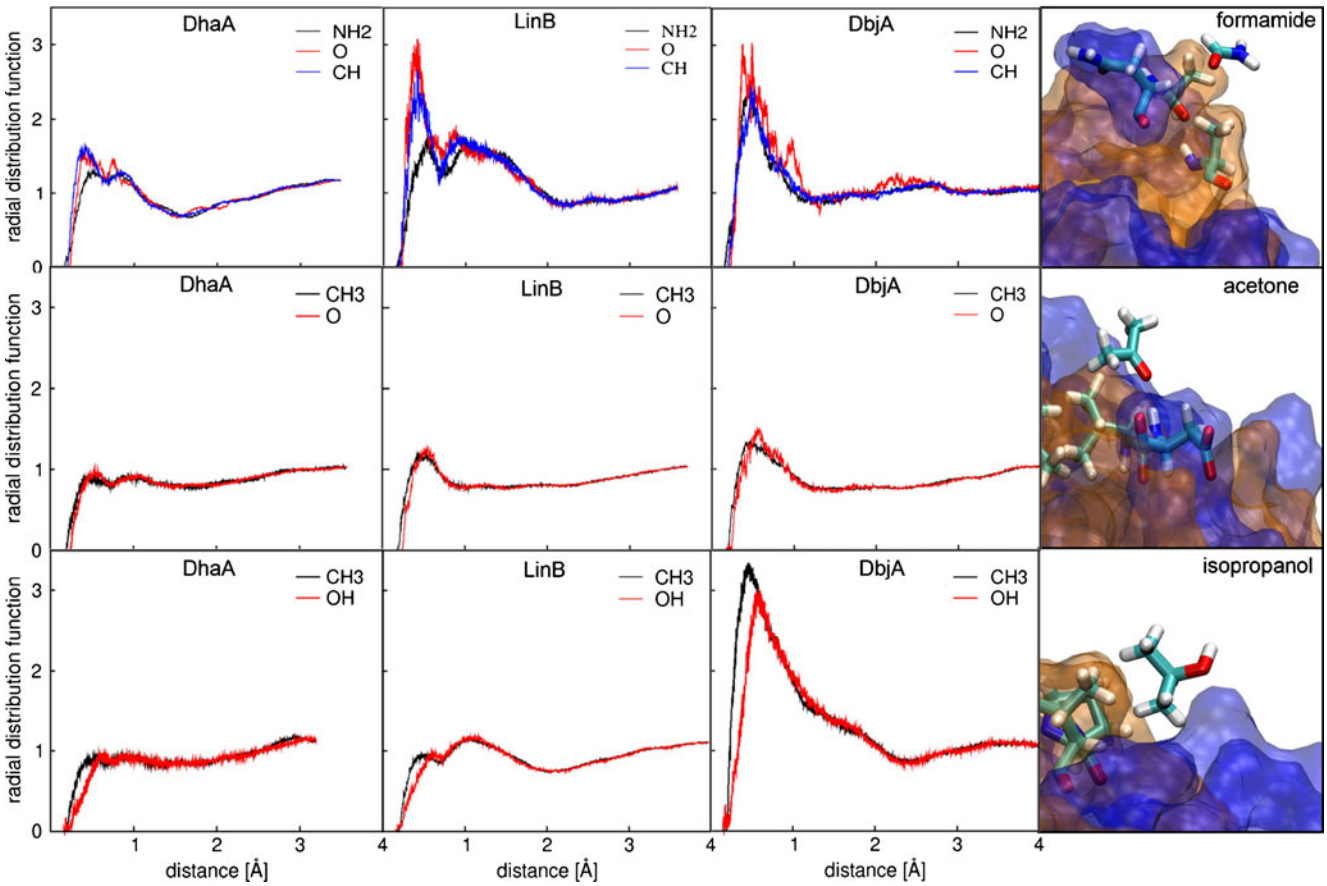

Fig. 3 Orientation of organic solvents on hydrophobic surfaces of HLDs. The radial distribution function (RDF) suggests that formamide oxygen and CH group are closer to the hydrophobic surface than the amide group (*first row*); the methyl group of acetone is closer than the oxygen group (*middle row*); and the methyl group of isopropanol is closer than the hydroxyl group (*bottom row*)

interface and our results are consistent with data at the air-water interface [43], which can be attributed to the much lower dielectric constant of the protein relative to the selected organic solvent. Depending on the distribution of charges on the surface, they can have different dielectric constants, with the dielectric constant of most globular protein surfaces being approximately 3-6, compared to high dielectric constant of water 80 [44]. Like acetone and formamide, also the RDF of isopropanol molecules (Fig. 3) in the vicinity of hydrophobic surface shows a similar behavior as observed at the air water interface [45], indicating that the isopropanol methyl groups are sticking to the enzymes hydrophobic patches while its OH group is pointing to the adjacent hydrophilic amino acids and/or the solution in which it interacts with water and/or isopropanol molecules.

Effects of organic solvents on tertiary protein structures

The effect of protein surface properties on the behavior of the organic solvent-water mixture at the surface of the enzymes described above alters structural and dynamical properties of all three HLDs enzymes. In the presence of organic solvents, the number of H-bonds between HLDs and water decreases, whereas the number of hydrogen bonds between protein and organic solvents increases (Table 3), indicating that the water molecules are actually repelled from the surface of the enzymes and replaced by co-solvent molecules. The average B-factor per residue was calculated from the last 5 ns of the simulations to evaluate the rigid and flexible regions of the three enzymes in different solvents. In almost all proteins, the rigidity of the small cap domain residues was altered by organic solvents (Fig. 4). In all solvents, the proteins display higher rigidity

Fig. 4 Average per-residue B-factors calculated from the last 5 ns of the simulations for HLDs in pure water and in organic solvents (*top*) and superimposed HLDs structures in water and organic solvents (*bottom*). Residues corresponding to the cap domain are shown in *yellow*. Parts of the structure with different B-factors in organic solvent are shown in *red*

in the core and the active site regions. The average structure of each protein obtained from the last 5 ns of the simulations in each solvent was superimposed onto each average structure in water to evaluate location of the solvent effects on the HLDs structure. B-factors for DhaA and its representative structure in formamide, acetone and isopropanol, indicate that the DhaA structure was either more rigid compared to LinB and DbjA, or its dynamics was not influenced by the presence of organic solvents (Fig. 4). The comparison of average structures of DhaA showed that formamide influenced mostly the helices α_5, α_8 and α_{11}, based on the nomenclature for the general topology of HLDs described by Janssen [5]. Acetone mainly affects the cap domain, since the whole α_4, α_5 helices, and part of α_8 helix were more stable. Similar to formamide and acetone, isopropanol altered the dynamic behavior of the DhaA cap domain. The main domain did not show any alterations in the isopropanol-water solution, where DhaA exhibits a structural flexibility and rigidity similar to the situation in pure water. Taking these results together leads to the conclusion that the DhaA structure is slightly more rigid in the presence of organic solvents. B-factors were also calculaculated for the dehalogenase LinB (Fig. 4). In the case of formamide, the linker connecting the cap domain with the main domain, and the loops located close to the tunnel opening in the cap domain, exhibited larger rigidity. The situation was different in acetone-water mixture. While the loops of the main domain loops are more

Table 3 Number of hydrogen bonds between DhaA, LinB, DbjA and organic solvents

Enzyme	Organic solvents	Protein-protein H-bond	Protein-water H-bond	Protein-organic molecules H-bond
DhaA	acetone	220±3	508±10	13±2
	isopropanol	225±3	502±9	16±3
	formamide	216±3	504±13	36±6
	water	212±4	548±10	NA
LinB	acetone	232±3	516±5	12
	isopropanol	228±2	535±6	15±3
	formamide	232±3	519±1	36±4
	water	229±2	565±1	NA
DbjA	acetone	234±5	438±12	11±2
	isopropanol	229±6	460±9	16±4
	formamide	231±3	453±8	42±7
	water	230±6	467±8	NA

NA – not applicable

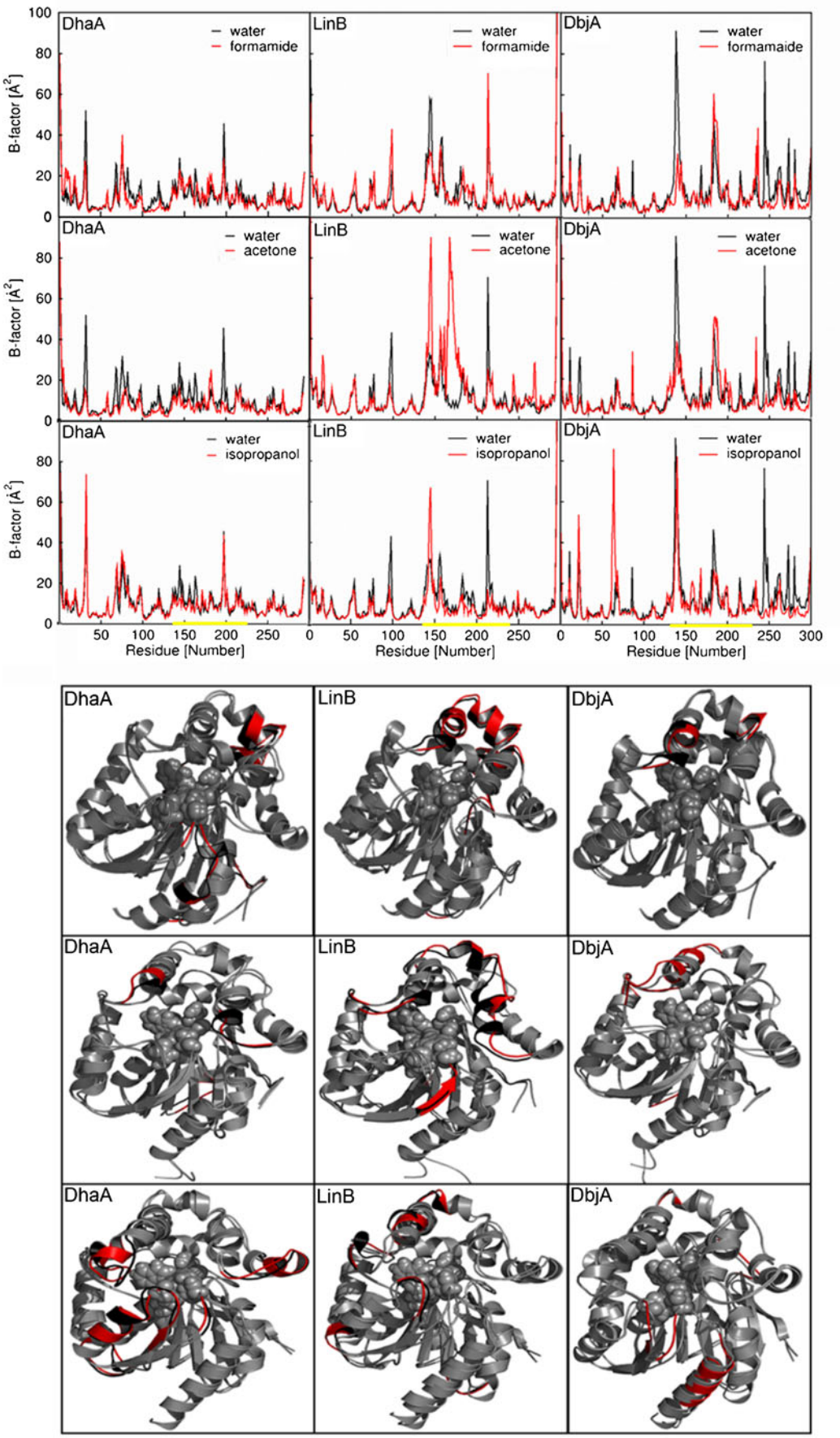
DhaA
LinB
DbjA
water
formamide
acetone
isopropanol
B-factor [Å²]
Residue [Number]

rigid, B-factors show high deviations for loops in the cap domain and those linking the main and the cap domain. In general, the cap domain was more flexible in acetone. In isopropanol, mainly loops on the cap domain and the linker are involved in the interaction with organic solvents. Organic solvents thus do not have an effect on the flexibility of the overall LinB structure, but some parts of the protein became more flexible, while other parts become either more stable or were not altered. In contrast to the two other HLDs, organic solvents influenced both domains of DbjA. Except one small part in the cap domain, the whole DbjA structure has less deviation than in formamide solution, as can be seen from the comparison of B-factor graphs in formamide and water (Fig. 4). Comparison of overall dehalogenase structures in both water and organic solvent solutions leads to the general conclusion that organic molecules stabilize the structures of these enzymes, with the exception of LinB in acetone.

Effects of organic solvents on quarternary protein structure

Among the three selected enzymes, DbjA is the only one which forms dimers (Fig. 1). Hence, the conformation of the dimeric enzyme might be more affected by solution properties. In homodimeric DbjA, two monomers interact via long helices located at the C-terminal. These two helices expose several hydrophobic residues on their surface. Figure 2 shows the population of the different solvents around and between the two monomers. Molecular dynamics simulations revealed that the organic solvents could penetrate between the two monomers. Since both acetone and isopropanol have the potential to make hydrophilic and hydrophobic interactions at the same time, they were trapped among the network of amino acids (Fig. 5). This network consists of six amino acids L51, P54, V55, L275, I273 and R292. Four of these amino acids belong to monomer A, and two of them belong to monomer B. Simulations in acetone solution showed that acetone molecules can penetrate to the network from both sides of the interface, and stayed there for the rest of the simulation time. In the case of the isopropanol solution, one isopropanol molecule penetrated to the network from one side, and stayed there for the whole simulation time, but isopropanol molecules approached the interface form the other side and exchanged with the bulk during the simulation (Fig. 6). To analyze the effect of trapped organic molecules on DbjA behavior, we measured the α angle between the long helices and the z axis (Fig. 1). Figure 7 shows the histogram of the angles adapted by the two monomers during the simulations. Alpha-angle of monomer A and B in water and formamide are almost the same. Throughout the simulation, the angles adopted by the monomers were in the range of 1–7 degree. In the case of acetone and isopropanol, the most frequently occurring angles were no longer similar for the two monomers due to the penetration of isopropanol and acetone molecules into the interface between the monomers. These molecules were locked in a fixed orientation between the two monomers via additional interactions, reducing mutual oscillations between the monomers. Ranges of angles reported in Fig. 7 show that the motion of both monomers was more restricted in acetone and isopropanol than in water and formamide. Since DbjA motion in acetone was locked by two acetone molecules, one from each side, the observed motion is significantly less pronounced than in the case of DbjA monomers in isopropanol.

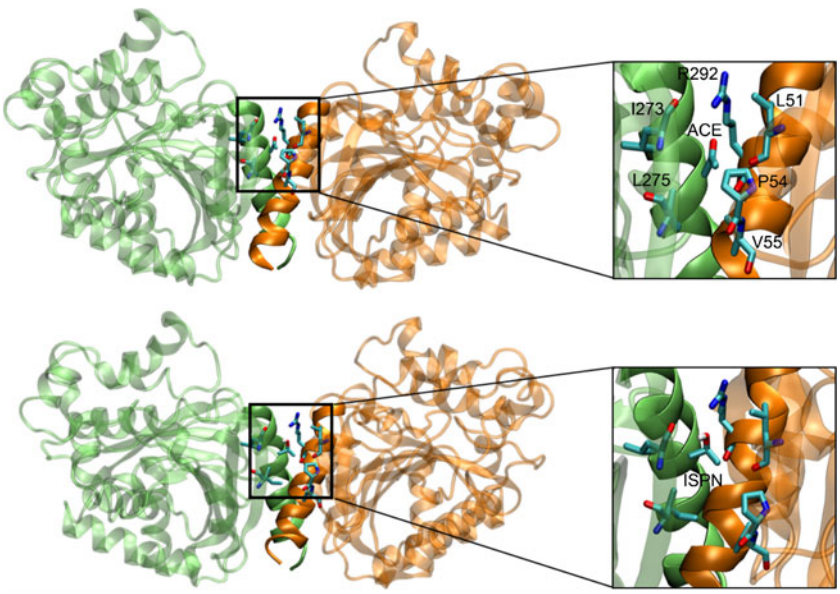

Fig. 5 Organic solvent molecules trapped inbetween monomer **a** (*green*) and monomer **b** (*orange*) of DbjA. Acetone (*top*) and isopropanol (*bottom*) molecules were localized in an analogous position and stabilized by the network of amino acids

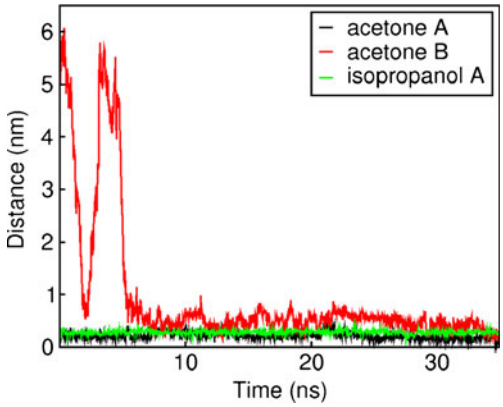

Fig. 6 Distance of selected acetone and isopropanol molecules from the center of the network of amino acids between two monomers of DbjA. Two acetone molecules and one isopropanol molecule were trapped during entire simulation within the monomer-monomer interface

Conclusions

The growing use of non-conventional solvent media in enzymatic biotechnological applications led to increasing interest in the behavior of protein structures in organic solvents. Three different HLDs (DhaA, LinB, and Dbja) and three different water-solvent environments (formamide, isopropanol and acetone) were used as model systems for analysis of distribution and orientation of solvent molecules at the protein interface. Since a protein surface has a low dielectric constant, the behavior of the organic solvents near the enzyme surface is similar to the behavior of organic solvents at the interface between air (with dielectric constant~1) and water. Formamide stays flat inbetween polar and non-polar parts of the enzyme surface, while both, acetone and isopropanol, mainly stick to non-polar areas of the surface with their methyl group facing these regions. Changes in the solvent-water layer around the protein lead to an alteration of the dynamical properties of the enzyme, and a change in B-factors. Hereby, mainly the cap domain is altered in DhaA and LinB, whereas in the case of DbjA, the main domain is mostly affected. Since DbjA is a dimeric structure, organic solvents have an additional effect on the monomer-monomer interaction. Physico-chemical properties of water and formamide are quite similar and therefore it is reasonable that the dihedral angle between monomer A and monomer B in formamide and water are only slightly different, while the nature of acetone and isopropanol leads to a significant increase in the angle between these two monomers. The penetration of acetone and isopropanol into the monomer-monomer interface restrains the mutual motion of both monomers. We might conclude that comparison and confrontation of our theoretical findings with experimental results for these three enzymes may give a useful approximation for generally relevant structural effects of organic solvents on enzyme surfaces, predictable from their and the protein surfaces physico-chemical properties.

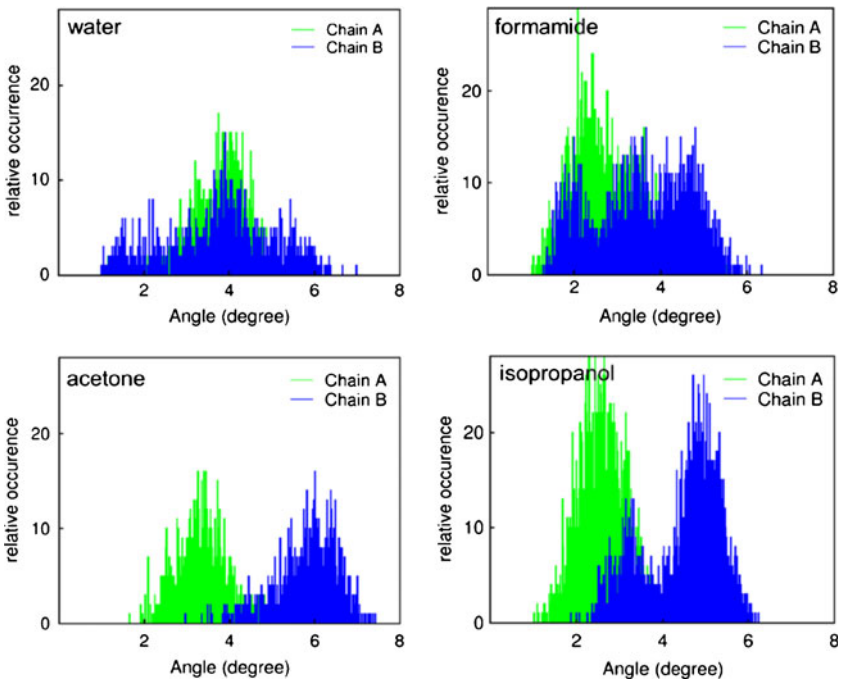

Fig. 7 Angle distribution of the helices involved in the intermonomer contact: monomers **a** (*green*) and monomer **b** (*blue*). The angle is measured between the z axis and the respective helices. The range in water and formamide is more widespread and shows fluctuations of both monomers toward each other. In the case of acetone and isopropanol, angle distributions are localized in the extreme of the fluctuations range

Acknowledgments M.K. and R.E. acknowledge support from the Czech Science Foundation, Grants 203/08/0114 and P207/10/1934, the Academy of Sciences of the Czech Republic, Grants AV0Z60870520 and IAA401630901, and the Ministry of Education, Youth and Sports of the Czech Republic, (projects No. ME09062 and MSM6007665808), and the European Regional Development Fund, Grants CZ.1.05/2.1.00/01.0001 and CZ.1.05/1.1.00/02.0123. Additionally, M.K. was supported by the University of South Bohemia, Grant GAJU 170/2010/P. Access to the National Grid Infrastructure -MetaCentrum- is highly appreciated

References

1. Fetzner S, Lingens F (1994) Bacterial dehalogenases: biochemistry, genetics, and biotechnological applications. Microbiol Mol Biol Rev 58:641–685
2. Damborský J, Rorije E, Jesenská A, Nagata Y, Klopman G, Peijnenburg WJ (2001) Structure-specificity relationships for haloalkane dehalogenases. Environ Toxicol Chem 20:2681–2689
3. Stucki G, Thueer M (1995) Experiences of a large-scale application of 1,2-dichloroethane degradation microorganisms for groundwater treatment. Environ Sci Technol 29:2339–2345
4. Ollis DL, Cheah E, Cygler M, Dijkstra B, Frolow F, Franken SM, Harel M, Remington SJ, Silman I, Schrag J (1992) The alpha/beta hydrolase fold. Protein Eng 5:197–211
5. Janssen DB (2004) Evolving haloalkane dehalogenases. Curr Opin Chem Biol 8:150–159
6. Chovancova E, Kosinski J, Bujnicki JM, Damborsky J (2007) Phylogenetic analysis of haloalkane dehalogenases. Proteins 67:305–316
7. Kaur J, Sharma R (2006) Directed evolution: an approach to engineer enzymes. Crit Rev Biotechnol 26:165–199
8. Prokop Z, Sato Y, Brezovsky J, Mozga T, Chaloupkova R, Koudelakova T, Jerabek P, Stepankova V, Natsume R, van Leeuwen JG, Janssen DB, Florian J, Nagata Y, Senda T, Damborsky J (2010) Enantioselectivity of haloalkane dehalogenases and its modulation by surface loop engineering. Angew Chem Int Ed Engl 49:6111–6115
9. Newman J, Peat TS, Richard R, Kan L, Swanson PE, Affholter JA, Holmes IH, Schindler JF, Unkefer CJ, Terwilliger TC (1999) Haloalkane dehalogenases: structure of a Rhodococcus enzyme. Biochemistry 38:16105–16114
10. Marek J, Vévodová J, Smatanová IK, Nagata Y, Svensson LA, Newman J, Takagi M, Damborský J (2000) Crystal structure of the haloalkane dehalogenase from *Sphingomonas paucimobilis* UT26. Biochemistry 39:14082–14086
11. Chaloupkova R, Sykorova J, Prokop Z, Jesenska A, Monincova M, Pavlova M, Tsuda M, Nagata Y, Damborsky J (2003) Modification of activity and specificity of haloalkane dehalogenase from *Sphingomonas paucimobilis* UT26 by engineering of its entrance tunnel. J Biol Chem 278:52622–52628
12. Štěpánková V, Khabiri M, Brezovský J, Pavelka A, Sýkora J, Amaro M, Minofar B, Prokop Z, Hof M, Ettrich R, Damborský J, Chaloupková R (2012) Expansion of tunnels and active-site cavities influence catalytic activity of haloalkane dehalogenases in organic co-solvents. *submitted*
13. Halling PJ (2004) What can we learn by studying enzymes in non-aqueous media? Philos Trans R Soc Lond B Biol Sci 359:1287–1296
14. Charles T (1973) The hydrophobic effect: formation of micelles and biological membranes. John Wiley & Sons, New York, p 220
15. Klibanov AM (2001) Improving enzymes by using them in organic solvents. Nature 409:241–246
16. Torres S, Castro G (2004) Non-aqueous biocatalysis in homogeneous solvent systems. Food Technol Biotechnol 42:271–277
17. Maurel P, Douzou P, Waldmann J, Yonetani T (1978) Enzyme behaviour and molecular environment. The effects of ionic strength, detergents, linear polyanions and phospholipids on the pH profile of soluble cytochrome oxidase. Biochim Biophys Acta 525:314–324
18. Yang L, Dordick JS, Garde S (2004) Hydration of enzyme in nonaqueous media is consistent with solvent dependence of its activity. Biophys J 87:812–821
19. Soares CM, Teixeira VH, Baptista AM (2003) Protein structure and dynamics in nonaqueous solvents: insights from molecular dynamics simulation studies. Biophys J 84:1628–1641
20. Hudson EP, Eppler RK, Clark DS (2005) Biocatalysis in semi-aqueous and nearly anhydrous conditions. Curr Opin Biotechnol 16:637–643
21. Micaêlo NM, Soares CM (2007) Modeling hydration mechanisms of enzymes in nonpolar and polar organic solvents. FEBS J 274:2424–2436
22. Serdakowski AL, Dordick JS (2008) Enzyme activation for organic solvents made easy. Trends Biotechnol 26:48–54
23. Boas FE, Harbury PB (2007) Potential energy functions for protein design. Curr Opin Struct Biol 17:199–204
24. Patargias GN, Harris SA, Harding JH (2010) A demonstration of the inhomogeneity of the local dielectric response of proteins by molecular dynamics simulations. J Chem Phys 132:235103–235111
25. Frisch MJ et al. (2004) Gaussian 03. Gaussian Inc, Wallingford
26. Horta BAC, Alencastro RBD, Ribeiro AAST (2008) MKTOP: a program for automatic construction of molecular topologies. J Braz Chem Soc 19:1433–1435
27. Bruice TC, Kahn K (2002) Parameterization of OPLS-AA force field for the conformational analysis of macrocyclic polyketides. J Comput Chem 23:977–996
28. Jorgensen WL, Maxwell DS, Tirado-Rives J (1996) Development and testing of the OPLS all-atom force field on conformational energetics and properties of organic liquids. J Am Chem Soc 118:11225–11236
29. Puhovski YP, Rode BM (1995) Structure and dynamics of liquid formamide. Chem Phys 190:61–82
30. Kulakova AN, Larkin MJ, Kulakov LA (1997) The plasmid-located haloalkane dehalogenase gene from *Rhodococcus rhodochrous* NCIMB 13064. Microbiology 143:109–115
31. Krieger E, Koraimann G, Vriend G (2002) Increasing the precision of comparative models with YASARA NOVA–a self-parameterizing force field. Proteins 47:393–402
32. Berendsen HJC, Grigera JR, Straatsma TP (1987) The missing term in effective pair potential. J Phys Chem 91:6269–6271
33. Berendsen HJC, van der Spoel D, van Drunen R (1995) GROMACS: a message-passing parallel molecular dynamics implementation. Comput Phys Commun 91:43–56
34. Lindahl E, Hess B, van der Spoel D (2001) GROMACS 3.0: a package for molecular simulation and trajectory analysis. J Mol Model 7:306–317
35. Berendsen HJC, Postma JPM, van Gunsteren WF, DiNola A, Haak JR (1984) Molecular dynamics with coupling to an external bath. J Chem Phys 81:3684–3690
36. Essmann U, Perera L, Berkowitz M (1995) A smooth particle mesh Ewald method. J Chem Phys 103:8577–8592
37. Hess B, Bekker H, Berendsen HJC, Fraaije JG (1997) LINCS: a linear constraint solver for molecular simulations. J Comput Chem 18:1463–1742
38. Humphrey W, Dalke A, Schulten K (1996) VMD-visual molecular dynamics. J Mol Graph 14:33–38
39. DeLano WL (2002) The PyMOL molecular graphics system. DeLano Scientific, San Carlos

40. Kovacs H, Mark AE, van Gunsteren WF (1997) Solvent structure at a hydrophobic protein surface. Proteins 27:395–404
41. Oberbrodhage J, Morgner H, Tapia O, Siegbahn HOG (1997) Molecular dynamics simulation of the free surface of liquid formamide. Int J Quantum Chem 63:1123–1131
42. Andersson G (2007) Angle resolved ion scattering spectroscopy at surfaces of pure liquids: topography and orientation of molecules. Phys Chem Chem Phys 7:2942–2947
43. Chen H, Gan W, Wu BH, Wu D, Guo Y, Wang HF (2005) Determination of structure and energetics for Gibbs surface adsorption layers of binary liquid mixture 1. Acetone+water. J Phys Chem B 109:8053–8063
44. Simonson T, Brooks LC (1996) Charge screening and the dielectric constant of proteins: Insights from molecular dynamics. J Am Chem Soc 118:8452–8458
45. Kataoka S (2006) Cremer PS Probing molecular structure at interfaces for comparison with bulk solution behavior: water/2-propanol mixtures monitored by vibrational sum frequency spectroscopy. J Am Chem Soc 128:5516–5522
46. Chovancová E, Pavelka A, Beneš P, Strnad O, Brezovský J, Kozlíková B, Gora A, Šustr V, Klvaňa M, Medek P, Biedermannová L, Sochor J, Damborský J (2012) CAVER 3.0: a tool for analysis of transport pathways in dynamic protein structures. PLOS Computational Biology, under review